Quantum Information and Computation, Vol. 14, No. 1&2 (2014) 0107–0121

NONLOCAL ENTANGLEMENT CONCENTRATION OF SEPARATE NITROGEN-VACANCY CENTERS COUPLING TO MICROTOROIDAL RESONATORS

CHUAN WANG YONG ZHANG MING LEI GUANG-SHENG JIN HAI-QIANG MA RU ZHANG
School of Science and State Key Laboratory of Information photonics and Optical Communications
Beijing University of Posts and Telecommunications,
Beijing, 100876, People's Republic of China

Received November 26, 2012
Revised May 6, 2013

Here we propose two practical protocols to concentrate entanglement between separate nitrogen-vacancy (N-V) centers in less entangled state via coupling to microtoroidal resonators. We construct the parity check gate of the N-V center and microtoroidal resonator systems via the interaction with the ancillary photon input-output process near the microtoroidal resonators. Thus the parity of the N-V center state can be readout by the measurement on the ancillary photon. Then we introduce the parity check operations to entanglement concentration protocols. Considering current techniques, we also discuss the feasibility of our proposal and its experimental challenges.

Keywords: Entanglement concentration, N-V centers, microtoroidal resonator.

Communicated by: S Braunstein & G Milburn

1. Introduction

Quantum entanglement plays an important role in the realization of quantum information processing (QIP). For example, quantum entanglement can be widely used in quantum communication [1, 2, 3, 4, 5], quantum teleportation [6] and distributed quantum computation. However, environment noise is a major obstacle in the realization of QIP which will reduce the fidelity of entanglement. In order to improve the entanglement fidelity of the quantum systems, the users can recur to entanglement concentration. In 1996, Bennett *et al.* [7] proposed an entanglement concentrate protocol (ECP) to distill a subset system in a maximally entangled state from a set of system in a less-entangled pure state. In 2000, Shi *et al.* [8] designed an ECP by using two-particle collective unitary evaluations. In 2001, Yamamoto *et al.* [9] proposed an ECP with polarization beam splitters. Later in 2003, Zhao [10] and Yamamoto [11] experimentally demonstrated the ECP using linear optics independently. In 2008, Sheng *et al.* [12] proposed an efficient ECP using cross-Kerr nonlinearities. Later, they designed an ECP for single-photon entangled systems [13]. In 2011, Wang *et al.* proposed an ECP protocol using the quantum dot and microcavity coupled system in which quantum spin entangled state can be distilled efficiently [14]. In 2012, the optimal protocol of ECP has been proposed with the help of cross-Kerr nonlinearities in which only one copy of the less entangled state is used, and the efficiency is improved [15, 16].

Nitrogen vacancy (N-V) center based solid state system is one of the most promising candidates for QIP. Compared with other artificial atoms, the N-V centers can be initialized, manipulated, and measured with high fidelity at room temperature, also it possesses long decoherence time. Many theoretical and experimental works have been devoted to the hybrid system that combines the solid-state qubit with the high Q cavity. Among the various proposals, N-V defect in diamond that combines with the whispering-gallery mode (WGM) system has emerged as a promising solid-state candidate in the realization of QIP, as the N-V centers possess long-lived spin triplet at room temperature [17] which provides us enough lift time for coherent manipulation. The cavity assistant quantum gate with input-out process was firstly proposed by Duan *et al.* in 2005 [18]. In 2009, An *et al.* [19] discussed the quantum information processes of a single photon interacted with a low-Q cavity. They proposed the dynamics of the single photon input-output processes. In 2010, Yang *et al.* [20] presented a protocol for W state and Bell state generation by using N-V centers coupled to whispering-gallery mode cavity. Also the proposed system can be generalized to quantum memories for quantum computation [21]. Dayan *et al.* illustrated the dynamics of a single atom coupled with a microcavity resonator [22], which indicates that the single atom within the resonator can dynamically control the cavity output. Later in 2011, Chen *et al.* [23] presented another entanglement generation protocol exploiting N-V centers via the coupling to microtoroidal resonators. Li *et al.* [24] proposed a quantum information transfer protocol with N-V centers coupled to whispering-gallery microresonator. In 2012, Yu *et al.* discussed the coupling of a high-Q WGM microresonator interacts with diamond nanocrystals theoretically, and claimed that the proposed system can be further applied for entanglement generation in QIP. Besides these theoretical works, a large number of experimental works have reported that N-V centers are useful resource which could be rapid and high fidelity readout of quantum information from them [26]. Entanglement between solid state systems, such as N-V centers, becomes an important resource for the realization of QIP. Also the entanglement generation process [27] on N-V centers and microcavity systems have been experimentally studied. And the preservation and concentration of entanglement between N-V centers is a potentially practical resource for long-distance entanglement and scalable QIP. Various types of qubits are being studied for QIP [28, 29]. Among these, superconducting qubits are another promising candidate for QIP, because these can be scalable and integrated into a chip, and can also interact well with NV centers [30, 31, 32]. Also superconducting circuits can have resonators, which can be coupled to artificial atoms, N-V centers, and other two level systems, exhibiting many novel phenomena [33, 34, 35, 36].

In this work we present two ECPs to concentrate the two separate N-V centers via the coupling with microtoroidal resonators. To do the job, we construct the parity check gate of N-V centers. By exploiting an ancillary photon which passed through the N-V center and microresonator system, the parity information of the composite N-V center system will be revealed by the output mode of the ancillary photon. By measuring the polarization of the photon, the less entangled state can be concentrated to the maximally entangled state.

The paper is organized as follows: in Sec.2, we first explain the basic principle of the input-output relation of N-V center and microtoroidal coupling system, then generalize it to parity check gate for two N-V centers. In Sec.3, we demonstrate the principle of ECP for N-V centers by using parity check gates. In Sec.4, we propose the protocol of single N-V center

assisted ECP for N-V centers. We show that only one pair of entangled particles is needed in the optimal protocol, and a higher success probability is obtained. In Sec.5, we discuss the experimental feasibilities of our protocol and calculate the success probability of the presented ECPs. And the last section is our discussion and summary.

2. Input-output relation of the N-V center and microtoroidal system

The N-V centers in diamond can be described by an additional electron which consists of a substitutional nitrogen atom and an adjacent vacancy. The ground state of the N-V center is a spin triplet state with the splitting at 2.87 GHz between the levels with $m_s = 0$ and $m_s = \pm 1$. The excited states are defined as $|A_2\rangle = |E_-\rangle|m_s = +1\rangle + |E_+\rangle|m_s = -1\rangle$, and $|A_1\rangle = |E_-\rangle|m_s = +1\rangle - |E_+\rangle|m_s = -1\rangle$, here $|E_\pm\rangle$ are the orbital states [27]. The spin-spin interaction splits the $|A_1\rangle$ and $|A_2\rangle$ states by a gap of 3.3 GHz. And the transitions of $|A_2\rangle \leftrightarrow |-1\rangle$ and $|A_2\rangle \leftrightarrow |+1\rangle$ can be realized by left and right circularly polarized photon excitation and decay in the limit of low strain [23]. The energy level structure with coupling to the cavity mode and driving laser fields of the N-V center is shown in figure 1. The quantum information is encoded in the spin state $|0\rangle = |m_s = -1\rangle$ and $|1\rangle = |m_s = +1\rangle$. The Λ type system could be realized in the N-V center if the excited state $|e\rangle$ is in the state $|A_2\rangle$. Thus in this proposed system, the electron spin can be entangled with the photon polarization. Recently, the Λ type transition was used for spin-photon interaction in experiment [37]. Also the two transitions of the N-V center that are assumed to couple to different counterpropagating mode pairs in the cavities are studied [38]. We consider the model that a single N-V center is coupled

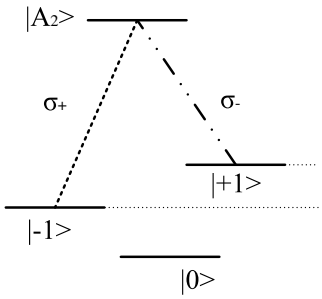

Fig. 1. The energy level structure of the N-V center coupling to microtoriodal cavity. Quantum information is encoded in the spin triplet state $|m_s = \pm 1\rangle$.

by the evanescent field of the microtoroidal resonator which is described by a single sided cavity. The N-V center and microtoroidal system have the following Hamiltonian under the Jaynes-Cummings model:

$$H = \sum_{i=1,2} [\frac{\hbar\omega_i}{2}\sigma_{i,z} + \hbar\omega_{c,i}a_i^\dagger a_i + i\hbar g_i(a_i\sigma_{i,+} - a_i^\dagger\sigma_{i,-})], \tag{1}$$

here a_i and $a_i^\dagger$ are the annihilation and creation operators of the cavity field of mode i. $\sigma_{i,z}$ represents the inversion operator of the N-V center with the mode i. $\sigma_{i,+}$ and $\sigma_{i,-}$ represent

the raising and lowering operators of the N-V center corresponding to mode i, respectively. The dynamics of the cavity field operator $\hat{a}$ and the operator σ_- can be written as [39]

$$\frac{d\hat{a}}{dt} = -[i(\omega_c - \omega_p) + \kappa + \frac{\kappa_s}{2}]\hat{a} - g\sigma_- - \sqrt{\kappa}\hat{a}_{in} + \hat{H}, \tag{2}$$

$$\frac{d\sigma_-}{dt} = -[i(\omega_0 - \omega_p) + \frac{\gamma}{2}]\sigma_- - g\sigma_z\hat{a} + \hat{G}, \tag{3}$$

here the coefficient g represents the coupling strength between the microcavity and N-V center. $\hat{\mathrm{H}}$ and $\hat{\mathrm{G}}$ are the noise operators related to reservoirs, $\gamma/2$ denotes the decay rate of the N-V center. κ and κ_s are the cavity decay rate and the cavity leaky rate, respectively. The frequencies of the input photon, cavity mode and the atomic level transition between the state $|-1\rangle$ and $|A_2\rangle$ are represented by ω_p, ω_c, ω_0, respectively. And the basic input-output relation for the N-V center and cavity coupled system has the following relation

$$a_{out}(t) = a_{in}(t) + \sqrt{\kappa}a(t). \tag{4}$$

The above Heisenberg equations of motion can be solved and the reflection coefficient of this system can be obtained [19, 39]:

$$r(\omega) = \frac{[i(\omega_0 - \omega_p) + \frac{\gamma}{2}][i(\omega_c - \omega_p) - \frac{\kappa}{2} + \frac{\kappa_s}{2}] + g^2}{[i(\omega_0 - \omega_p) + \frac{\gamma}{2}][i(\omega_c - \omega_p) + \frac{\kappa}{2} + \frac{\kappa_s}{2}] + g^2}. \tag{5}$$

On the resonant condition of the system with $\omega_c = \omega_p = \omega_0$, by taking $g = 0$, the the reflection coefficient r for the uncoupled cavity system can be written as

$$r_0(\omega) = \frac{i(\omega_c - \omega_p) + \frac{\kappa_s}{2} - \frac{\kappa}{2}}{i(\omega_c - \omega_p) + \frac{\kappa_s}{2} + \frac{\kappa}{2}}. \tag{6}$$

Figures 2 describes the numerical results for the coefficient of reflection versus the coupling strength. As illustrated in figure 2, if we choose the resonant condition, the reflectance is approach to unity as the coupling strength g/κ is larger than 3. For more general cases, we plot figure 3 for the absolute value of the reflection coefficient versus frequency detuning. We can conclude that we have $|r| = 1$ when there are large detunings between the cavity mode and the N-V centers.

To explain the mechanism of the interaction, we may consider the N-V center is prepared in the state $|-1\rangle$, the transition will be driven by the left circularly polarized photon in the state $|L\rangle$. And the output photon pulse can be described by $|\Phi_{out}\rangle = r(\omega)|L\rangle = e^{i\phi}|L\rangle$, here the parameter ϕ represents the phase shift determined by the input-output relation. However, if the input photon is prepared in the right circularly polarized state $|R\rangle$, the output photon will evolve as $|\Phi_{out}\rangle = r(\omega)|R\rangle = e^{i\phi_0}|R\rangle$, for ϕ_0 represents the randomly phase shift. Similarly, for an input linearly polarized photon in the state $\frac{1}{\sqrt{2}}(|L\rangle + |R\rangle)$, here the state $|L\rangle$ and $|R\rangle$ represent the left and right circularly polarized photon, respectively. The state of the output photon can be described by:

$$|\Psi_{out}\rangle = \frac{1}{\sqrt{2}}(e^{i\phi}|L\rangle + e^{i\phi_0}|R\rangle). \tag{7}$$

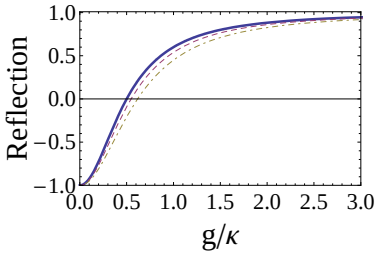

Fig. 2. The relation of reflectance and the coupling strength. Here the dipole decay rate γ/κ is 0.25 for the solid line. The dashed and dot-dashed lines represent the reflectance with the dipole decay rate γ/κ equal to 0.3 and 0.38, respectively.

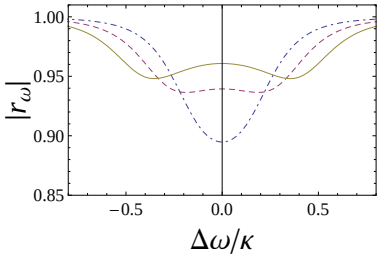

Fig. 3. The reflectance of the cavity versus the frequency detuning. Here the dipole decay rate γ/κ is 0.02. The coupling strength of the N-V center with the cavity is $g/\kappa = 0.3$, $g/\kappa = 0.4$ and $g/\kappa = 0.5$ for the dot-dashed line, dashed line and the solid line, respectively.

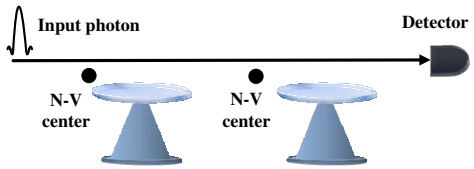

Fig. 4. The schematics diagram of the principle of parity check gate. The two N-V centers are coupled with microtoroidal resonators. One input photon is sent into the cavity and detected by the user.

The N-V center and microtoroidal system can be further generalized to realize the parity check gate (PCG) as the phase of the state can be readout without destroying the spins. The principle of PCG is shown in figure 4. The purpose of PCG is to readout the spin parity information of the particles without destroying them. The input photon is prepared in the state $(|L\rangle + |R\rangle)/\sqrt{2}$. Following the principle of interaction between the input photon and the N-V center and microtoroidal resonator, the process of parity check on N-V centers can be described as

$$\begin{aligned}\prod_p |+1\rangle|+1\rangle\frac{|L\rangle+|R\rangle}{\sqrt{2}} &\Rightarrow |+1\rangle|+1\rangle\frac{e^{2i\phi}|L\rangle+e^{2i\phi_0}|R\rangle}{\sqrt{2}}\\ \prod_p |-1\rangle|-1\rangle\frac{|L\rangle+|R\rangle}{\sqrt{2}} &\Rightarrow |+1\rangle|+1\rangle\frac{e^{2i\phi_0}|L\rangle+e^{2i\phi}|R\rangle}{\sqrt{2}},\end{aligned} \tag{8}$$

if the two N-V centers have the even parity.

However, if the two N-V centers are in the odd parity, the parity check process can be described by

$$\begin{aligned}\prod_p |+1\rangle|-1\rangle\frac{|L\rangle+|R\rangle}{\sqrt{2}} &\Rightarrow |+1\rangle|-1\rangle\frac{e^{i\phi+i\phi_0}(|L\rangle+|R\rangle)}{\sqrt{2}},\\ \prod_p |-1\rangle|+1\rangle\frac{|L\rangle+|R\rangle}{\sqrt{2}} &\Rightarrow |-1\rangle|+1\rangle\frac{e^{i\phi+i\phi_0}(|L\rangle+|R\rangle)}{\sqrt{2}}.\end{aligned} \tag{9}$$

Here we assume that the two phases ϕ and ϕ_0 are π and $\pi/2$, respectively. Then the output photon can be described by two orthogonal basis. For instance, the photon in the state $\frac{|L\rangle+|R\rangle}{\sqrt{2}}$ reveals that the spin parity of the two N-V centers is odd. However, the photon in the state $\frac{|L\rangle-|R\rangle}{\sqrt{2}}$ represents that the parity of the N-V centers is even. By measuring the polarization state of the ancillary photon, the parity of the two N-V centers can be readout. The above process describes the PCG operation of the two N-V centers spins.

3. Entanglement concentration using parity check gate for partially entangled pairs

We discussed the parity check process on the spin of N-V centers in the above section. Here we will generalize the PCGs to implement our ECP for N-V centers. And the basic principle of the ECP using N-V centers and microtoroidal resonators is shown in figure 5. The less entangled N-V centers are shared between Alice and Bob. The two pairs of entangled N-V centers can be described by the following state:

$$|\phi^+\rangle_{a,b} = \alpha|+1\rangle_a|+1\rangle_b + \beta|-1\rangle_a|-1\rangle_b. \tag{10}$$

The single ancillary photon is prepared in the state $|\psi_p\rangle = \frac{1}{\sqrt{2}}(|R\rangle + |L\rangle)$. Then Bob perform the PCG operation on his two particles. Following the principles shown in figure 5, the photon interacts with the N-V centers b_1 and b_2, respectively, and the system evolves as follows:

$$|\phi_1^+\rangle|\phi_2^+\rangle|\psi_p\rangle$$

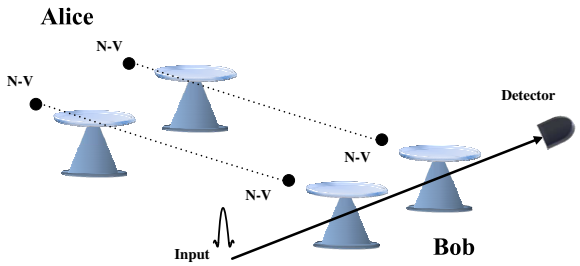

Fig. 5. The schematics diagram of the principle of entanglement concentration between entangled N-V centers non-locally. The dotted line represents the entanglement between N-V centers. Here the N-V centers are fixed on the exterior surface of the microtoroidal resonators via single photon input and output. The single photon with circularly polarized state is sent into the input port.

$$
\begin{aligned}
= \quad & [\alpha^2|+1\rangle_{a_1}|+1\rangle_{b_1}|+1\rangle_{a_2}|+1\rangle_{b_2} + \beta^2|-1\rangle_{a_1}|-1\rangle_{b_1}|-1\rangle_{a_2}|-1\rangle_{b_2} \\
& + \ \alpha\beta(|+1\rangle_{a_1}|+1\rangle_{b_1}|-1\rangle_{a_2}|-1\rangle_{b_2} + |-1\rangle_{a_1}|-1\rangle_{b_1}|+1\rangle_{a_2}|+1\rangle_{b_2})]|\psi\rangle_p \\
\Rightarrow \quad & \alpha^2|+1\rangle_{a_1}|+1\rangle_{b_1}|+1\rangle_{a_2}|+1\rangle_{b_2} \otimes (|L\rangle e^{i\phi_0+i\phi_0'} + |R\rangle e^{i\phi+i\phi'}) \\
& +\beta^2|-1\rangle_{a_1}|-1\rangle_{b_1}|-1\rangle_{a_2}|-1\rangle_{b_2} \otimes (|L\rangle e^{i\phi+i\phi'} + |R\rangle e^{i\phi_0+i\phi_0'}) \\
& +\alpha\beta|+1\rangle_{a_1}|+1\rangle_{b_1}|-1\rangle_{a_2}|-1\rangle_{b_2} \otimes (|L\rangle e^{i\phi_0+i\phi'} + |R\rangle e^{i\phi+i\phi_0'}) \\
& +\alpha\beta|-1\rangle_{a_1}|-1\rangle_{b_1}|+1\rangle_{a_2}|+1\rangle_{b_2} \otimes (|L\rangle e^{i\phi+i\phi_0'} + |R\rangle e^{i\phi_0+i\phi'}). \qquad (11)
\end{aligned}
$$

Then Bob measures the polarization of the ancillary photon. Consider the resonant condition $\omega_c = \omega_0 = \omega_p$, we have the relation $\phi_0 = \phi_0^{'} = \pi/2$, and $\phi = \phi^{'} = \pi$. If the single photon is detected in the state $(|R\rangle + |L\rangle)/\sqrt{2}$, the state of the remaining four spins becomes

$$
\frac{1}{\sqrt{2}}(|+1\rangle_{a_1}|+1\rangle_{b_1}|-1\rangle_{a_2}|-1\rangle_{b_2} + |-1\rangle_{a_1}|-1\rangle_{b_1}|+1\rangle_{a_2}|+1\rangle_{b_2}). \qquad (12)
$$

Then the two non-local parties perform single qubit spin flip operation of the N-V centers marked with a_2 and b_2. The single qubit flip operation will transform the state to

$$
\frac{1}{\sqrt{2}}(|+1\rangle_{a_1}|+1\rangle_{b_1}|+1\rangle_{a_2}|+1\rangle_{b_2} + |-1\rangle_{a_1}|-1\rangle_{b_1}|-1\rangle_{a_2}|-1\rangle_{b_2}). \qquad (13)
$$

Both of them perform the X-basis measurement on the N-V centers a_2 and b_2, respectively, the four-spin entangled state can be expanded by the form

$$
\begin{aligned}
& \frac{1}{2\sqrt{2}}[|+1\rangle_{a_1}|+1\rangle_{b_1} \otimes (|+X\rangle + |-X\rangle)_{a_2} \\
& \otimes \ (|+X\rangle + |-X\rangle)_{b_2} + |-1\rangle_{a_1}|-1\rangle_{b_1} \\
& \otimes \ (|+X\rangle - |-X\rangle)_{a_2} \otimes (|+X\rangle - |-X\rangle)_{b_2}] \\
= \quad & \frac{1}{2}|\phi^+\rangle_{a_1,b_1}(|+X\rangle_{a_2}|+X\rangle_{b_2} + |-X\rangle_{a_2}|-X\rangle_{b_2}) \\
& + \ \frac{1}{2}|\phi^-\rangle_{a_1,b_1}(|+X\rangle_{a_2}|-X\rangle_{b_2} + |-X\rangle_{a_2}|+X\rangle_{b_2}). \qquad (14)
\end{aligned}
$$

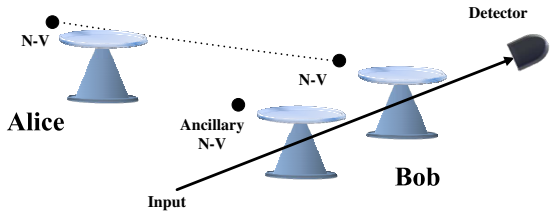

Fig. 6. The schematics diagram of the principle of efficient entanglement concentration between one entangled N-V centers non-locally. Here the ancillary N-V center is used. The single photon with circularly polarized state is sent through the input port.

We can conclude that if the results of the spins have the even parity (both in the $|+X\rangle$ state or in the $|-X\rangle$ state), then the remaining two N-V centers can be concentrated into the maximally entangled state $|\phi^+\rangle$, otherwise the two N-V centers are in the odd parity, they can confirm that the remaining state can be described by $|\phi^-\rangle$.

The efficiency of the proposed ECP based on N-V centers has the same efficiency as that for entangled photon pairs based on linear optics [12]. The yield of maximally entangled states can be described by the probability as $2|\alpha\beta|^2$ which is the ratio of the number of maximally entangled pairs and the number of originally less entangled pairs.

4. Efficient single N-V center assisted entanglement concentration for partially entangled N-V centers

Compared with the previous protocols, the two parties need two pairs of entangled state in order to get one pair of maximally entangled state. However, if the user knows the probability amplitude of the state, then the ECP can be realized by only one pair of less entangled state. Here in this section, we propose a more economical protocol which requires only one pair of less-entangled state and one ancillary electron spin in N-V center.

The basic principle of our ECP protocol is shown in figure 6. The pure less entangled state shared by the two parties Alice and Bob is described by the following state:

$$|\phi^+\rangle_{a,b} = \alpha|+1\rangle_a|+1\rangle_b + \beta|-1\rangle_a|-1\rangle_b, \tag{15}$$

here the coefficients $|\alpha|^2 + |\beta|^2 = 1$. The initial state of the ancillary N-V center is prepared in the state

$$|\chi\rangle_{b_1} = \alpha|+1\rangle_{b_1} + \beta|-1\rangle_{b_1}. \tag{16}$$

The state of the three-particle N-V center system can be described as

$$\begin{aligned} |\Psi\rangle = \quad & |\phi^+\rangle_{a,b}|\chi\rangle_{b_1} \\ = \quad & \alpha^2|+1\rangle|+1\rangle|+1\rangle + \beta^2|-1\rangle|-1\rangle|-1\rangle \\ & + \ \alpha\beta(|+1\rangle|+1\rangle|-1\rangle + |-1\rangle|-1\rangle|+1\rangle). \end{aligned} \tag{17}$$

Exploiting the setup shown in figure 6, the evolution of the composite system by employing the ancillary photon in the state $|\psi\rangle_p = \frac{1}{\sqrt{2}}(|L\rangle + |R\rangle)$ can be described as follows:

$$\begin{aligned} & [\alpha^2|+1\rangle|+1\rangle|+1\rangle + \beta^2|-1\rangle|-1\rangle|-1\rangle \\ & + \ \alpha\beta(|+1\rangle|+1\rangle|-1\rangle + |-1\rangle|-1\rangle|+1\rangle)]|\psi\rangle_p \\ \Rightarrow \ & \alpha^2|+1\rangle_a|+1\rangle_b|+1\rangle_{b_1}(|L\rangle e^{i\phi_0+i\phi_0'} + |R\rangle e^{i\phi+i\phi'}) \\ & + \ \beta^2|-1\rangle_a|-1\rangle_b|-1\rangle_{b_1}(|L\rangle e^{i\phi+i\phi'} + |R\rangle e^{i\phi_0+i\phi_0'}) \\ & + \ \alpha\beta|+1\rangle_a|+1\rangle_b|-1\rangle_{b_1}(|L\rangle e^{i\phi_0+i\phi'} + |R\rangle e^{i\phi+i\phi_0'}) \\ & + \ \alpha\beta|-1\rangle_a|-1\rangle_b|+1\rangle_{b_1}(|L\rangle e^{i\phi+i\phi_0'} + |R\rangle e^{i\phi_0+i\phi'}). \end{aligned} \tag{18}$$

Here we assume the relation $\phi_0 = \phi_0' = \pi/2$, and $\phi = \phi' = \pi$. By performing single photon measurement on the ancillary photon, if the state of the ancillary photon is in the state $\frac{1}{\sqrt{2}}(|R\rangle + |L\rangle)$, the three particles state collapses to:

$$\alpha^2|+1\rangle_a|+1\rangle_b|+1\rangle_{b_1} + \beta^2|-1\rangle_a|-1\rangle_b|-1\rangle_{b_1}. \tag{19}$$

Otherwise the remaining three particles state can be described by the following expression:

$$\frac{1}{\sqrt{2}}(|+1\rangle_a|+1\rangle_b|-1\rangle_{b_1} + |-1\rangle_a|-1\rangle_b|+1\rangle_{b_1}). \tag{20}$$

Then Bob measures the ancillary N-V center in the basis $|\pm X\rangle = \frac{1}{\sqrt{2}}(|+1\rangle \pm |-1\rangle)$. Equation (20) collapses to $\frac{1}{\sqrt{2}}(|+1\rangle_a|+1\rangle_b + |-1\rangle_a|-1\rangle_b)$ if the result of the measurement is $|+X\rangle$ and collapses to $\frac{1}{\sqrt{2}}(|+1\rangle_a|+1\rangle_b - |-1\rangle_a|-1\rangle_b)$ if the ancillary N-V center is in the state $|-X\rangle$.

For the other two items, the two N-V centers are in the state $\alpha^2|+1\rangle_a|+1\rangle_b+\beta^2|-1\rangle_a|-1\rangle_b$ or $\alpha^2|+1\rangle_a|+1\rangle_b - \beta^2|-1\rangle_a|-1\rangle_b$. These remaining states can also be concentrated into maximally entangled state by the iteration of the above processes. Here we assume that the two N-V centers are in the state $\alpha^2|+1\rangle_a|+1\rangle_b + \beta^2|-1\rangle_a|-1\rangle_b$, then Alice prepares a new ancillary N-V center in the state $\alpha^2|+1\rangle_{a_1} + \beta^2|-1\rangle_{b_1}$.

By repeating the concentration process, the state of the composite system can be described by

$$\begin{aligned} & [\alpha^4|+1\rangle|+1\rangle|+1\rangle + \beta^4|-1\rangle|-1\rangle|-1\rangle \\ & + \ \alpha^2\beta^2(|+1\rangle|+1\rangle|-1\rangle + |-1\rangle|-1\rangle|+1\rangle)]|\psi\rangle_p \\ \Rightarrow \ & \alpha^4|+1\rangle_a|+1\rangle_b|+1\rangle_{b_1}(|L\rangle e^{i\phi_0+i\phi_0'} + |R\rangle e^{i\phi+i\phi'}) \\ & + \ \beta^4|-1\rangle_a|-1\rangle_b|-1\rangle_{b_1}(|L\rangle e^{i\phi+i\phi'} + |R\rangle e^{i\phi_0+i\phi_0'}) \\ & + \ \alpha^2\beta^2|+1\rangle_a|+1\rangle_b|-1\rangle_{b_1}(|L\rangle e^{i\phi_0+i\phi'} + |R\rangle e^{i\phi+i\phi_0'}) \\ & + \ \alpha^2\beta^2|-1\rangle_a|-1\rangle_b|+1\rangle_{b_1}(|L\rangle e^{i\phi+i\phi_0'} + |R\rangle e^{i\phi_0+i\phi'}). \end{aligned} \tag{21}$$

We set the phases as $\phi_0 = \phi_0' = \pi/2$, and $\phi = \phi' = \pi$, then Alice and Bob keep the case when Bob's measurement on the single photon with the result $\frac{1}{\sqrt{2}}(|R\rangle + |L\rangle)$. Then by applying single electron spin rotation and measurement on the ancillary N-V center, Alice and Bob can recover the maximally entangled state between the remote N-V centers. Thus, the maximally

entangled state can be shared between them. The success probability of the ECP can be described by

$$P_1 = \frac{2|\alpha\beta|^4}{|\alpha|^4 + |\beta|^4}, \tag{22}$$

which is similar with the results in Ref.[15, 16].

The remaining N-V centers are in the state $\alpha^4|+1\rangle_a|+1\rangle_b + \beta^4|-1\rangle_a|-1\rangle_b$ or $\alpha^4|+1\rangle_a|+1\rangle_b - \beta^4|-1\rangle_a|-1\rangle_b$. Alice and Bob repeat the above processes. Then the two users can get the maximally entangled state from the remaining state with probability

$$P_2 = \frac{2|\alpha\beta|^8}{|\alpha|^8 + |\beta|^8}. \tag{23}$$

So we can conclude that the total success probability of the ECP after the iterated process can be represented by

$$P = 2|\alpha\beta|^2 + \frac{2|\alpha\beta|^4}{|\alpha|^4 + |\beta|^4} + \frac{2|\alpha\beta|^8}{|\alpha|^8 + |\beta|^8} + \cdots + \frac{2|\alpha\beta|^{2^n}}{|\alpha|^{2^n} + |\beta|^{2^n}}. \tag{24}$$

As the iterated time n is increased, the success probability of ECP approaches to unity. Thus far, we have fully described the ECP protocol on N-V centers via coupling to microtoroidal resonators.

5. Efficiencies of ECPs and Experiment feasibility

During the ECP process, we exploit the N-V centers and microtoroidal resonator coupling system to construct the PCGs. The key technologies of the realization are the coherent coupling between N-V center and the microtoroidal resonator. The efficiencies of ECPs may be effected by the decoherence of the N-V centers, the coupling strength and the cavity leakage. The solid state qubits may interacted with the environment and lost the entanglement. This effect requires the dynamics decoupling processes of the N-V centers [40]. Here we only focus on the effect of the coupling strength and the cavity leakage. Without loss of generality, we consider two entangled N-V centers with identical parameters coupled with microtoroidal resonators and verify the efficiencies of these schemes through numerical simulations.

In order to visualize the effect of the coupling constant g/κ and the frequencies detuning $\omega_c - \omega_p$, we have plotted in figure 7(a) the relation between the coefficient α of the initial partially entangled state and the coupling constant g/κ and the total success probability P of the first protocol. It is obvious that the success probability is relative to the entanglement of the initial state, and increases with the entanglement of the initial state. The success probability approaches to the maximal value when $\alpha = 1/\sqrt{2}$. Also figure 7(b) describes the relation between the success probability and the frequencies detuning and the initial entanglement.

Figure 8 illustrates the success probability of the second ECP. By iteration of the PCG operations, the success probability is larger than the traditional ECP. Here in figure 8(a) the dipole decay rate $\gamma/\kappa = 0.5$, the cavity is assumed to be ideal with no cavity leakage $\kappa_s/\kappa = 0.01$. The success probability of the ECP increases with the increment of the coupling strength and has the highest success probability as g/κ is larger than 2. Also the success

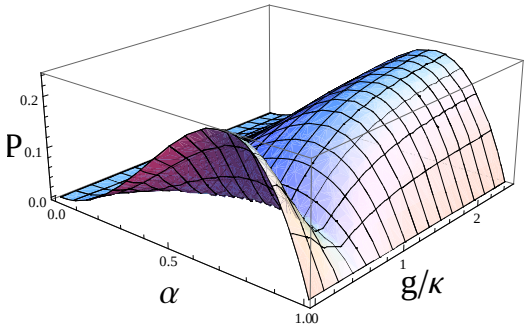

(a) The success probability of the first ECP versus the coupling strength and the coefficient α. Here the cavity leakage $\kappa_s/\kappa = 0.01$.

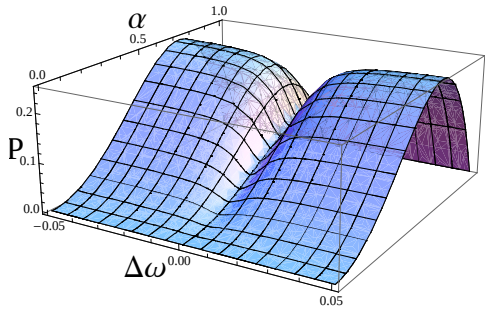

(b) The success probability of the first ECP versus the frequency detuning and the coefficient α.

Fig. 7. The success probabilities of ECPs versus the coupling strength and the frequencies detuning of the first ECP. Here we assume the ideal case of the cavity with the leakage $\kappa_s = 0$ and the dipole decay rate is $\gamma/\kappa = 0.05$.

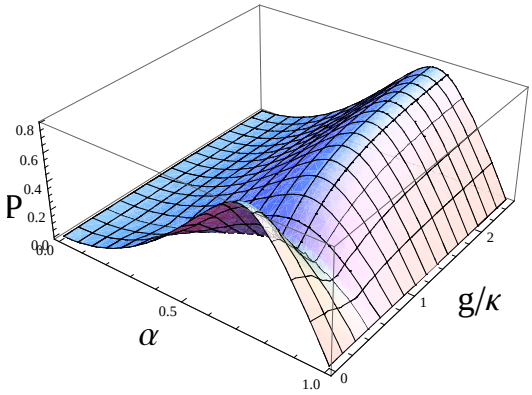

(a) The success probability of the second ECP versus the coupling strength and the coefficient α. Here we assume the cavity with the leakage $\kappa_s/\kappa = 0.01$.

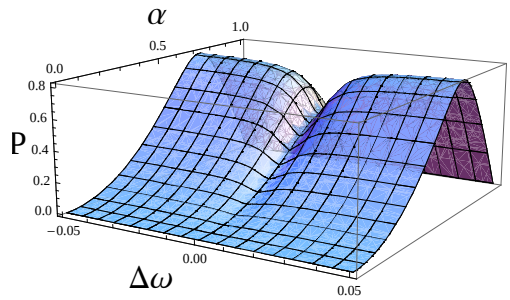

(b) The success probability of the second ECP versus the frequency detuning and the coefficient α.

Fig. 8. The success probabilities of ECPs versus the coupling strength and the frequencies detuning of the second ECP. Here the dipole decay rate is $\gamma/\kappa = 0.5$.

probabilities are affected by the detuning of the cavity field frequency and the rotating frame frequency.

For the implementation of this protocol, practical achievements in experiment with NV-centers and microtoroidal resonators can be used. N-V centers are well suited for QIP as qubits because they have long coherence electron spin relaxation time [17]. Also the electronic spins are easy for initialization, manipulation and measurement. Another key ingredient of our protocol is the coupling between N-V centers and various microcavity which have been studied by many groups, and the coupling strength of the N-V center with microcavity resonator is on the order of hundreds of megahertz. Strong coupling between a single N-V center and silica microsphere [41] and a gallium phosphide microdisc [42] has been reported. For instance in Ref.[42], the N-V centers are experimentally coupled with chip-based microcavity with $Q > 25,000$ and the coupling strength between a single microdisk photon and the N-V center zero photon line is $g/2\pi = 0.3GHz$. The total spontaneous emission rates of the N-V center is $\gamma/2\pi = 0.013GHz$.

Recently, the large coupling between N-V centers and photonic crystal nanocavity has been reached [43], also the realization of coupling between a frequency tunable superconducting resonator and an ensemble of N-V centers are realized [44]. Coherent coupling between N-V centers and microtoroidal resonator has been realized experimentally. For instance in [45], the coherent coupling rate of the N-V center zero photon line with the microdisk is $28MHz$ by placing the N-V center with 100-nanometer-scale in the near-field of a microdisk cavity using a fiber taper. In addition, the spin decoherence may also reduce the success probability of our proposed ECP. The main parameters of decoherence are characterized by spin relaxation time T_1 and dephasing time T_2. As discussed in Ref.[46], the electron spin relaxation time T_1 of N-V centers in diamond scales from microseconds to seconds at low temperature. Moreover, the dephasing time of N-V center is about 2ms in a isotopically pure diamond [47] which provides our scheme enough time for gate operations.

In all, the current experiment processes on N-V centers and microcavity system provide a platform for on-chip integration of multiple devices required by applications in quantum information processing. The setup designed here can be employed to study the general cases. One can apply the PCG operation to study the multi-particle entanglement concentration by extending the N-V centers system to n N-V centers coupled with microtoroidal resonators. Also the proposed setup provides a method to realize the entanglement transfer between photons and electron spin in N-V centers. Based on the ideas, we can build quantum repeaters between remote N-V centers, in which the N-V center and mirotoroidal unit plays the role of a quantum node in long distance quantum communication.

6. Summary

In summary, we have presented two protocols to concentrate two distant N-V centers fixed on the exterior surface of microtoroital which are in less entangled state. The two distant parties can obtain a maximally entangled state from less entangled N-V center particles, which will improve the efficiency of long-distance quantum information processing. In 2012, we have proposed an entanglement purification protocol using N-V centers and microtoroidal resonators [48]. The main purpose of purification is to purify entangled state from a mixed state ensemble which is different with the entanglement concentration processes.

In the realization of our protocols, we present a PCG operation based on N-V centers and microtoroital resonators. The PCG operation can distinguish the state parity of the N-V centers without destroying them. Then we propose two ECPs using PCGs. The ECPs require only single particle rotation and measurements. The first ECP employs two pairs of less entangled N-V centers to concentrate one pair N-V centers state to maximally entangled state. And the second ECP exploits one pair of less entangled N-V centers and one ancillary N-V center. The second protocol is more efficient as only one pair is needed. Then we discussed the success probabilities of the two protocols by using current experimental parameters.

Also, the protocols proposed here are easy to realize as only single photon detections are required. The N-V centers are optically addressable and can exhibit electron spin coherence lifetimes exceeding 1 *ms* at room temperature. The N-V centers and microtoroidal resonators system can be used to check the parity of entangled N-V center spins. In our proposed protocol, the state of the spins are not needed to be measured, so it is more flexible and require less resources.

Acknowledgements

This work is supported by the National Fundamental Research Program Grant No. 2010CB923202, Specialized Research Fund for the Doctoral Program of Education Ministry of China No. 20090005120008, the Fundamental Research Funds for the Central Universities, and China National Natural Science Foundation Grant Nos. 61205117 and 51102019.

References

1. Bennett C H, Brassard G and Mermin N D 1992 Phys. Rev. Lett. **68**, 557.
2. Briegel H J, Dür W, Cirac J I and Zoller P 2000 Phys. Rev. Lett. **81**, 5932-5935.
3. Duan L M, Lukin M D, Cirac J I and Zoller P 2001 Nature, 414, 413.
4. Long G L and Liu X S 2002 Phys. Rev. A **65**, 032302.
5. Deng F G, Long G L and Liu X S 2003 Phys. Rev. A **68**, 042317.
6. Bouwmeester D, Pan J W, Mattle K, Eibl M, Weinfurter H and Zeilinger A 1997 Nature **390**, 575.
7. Bennett C H, Bernstein H J, Popescu S and Schumacher B 1996 Phys. Rev. A **53**, 2046.
8. Shi B S, Jiang Y K and Guo G C 2000 Phys. Rev. A **62**, 054301.
9. Yamamoto T, Koashi M and Imoto N 2001 Phys. Rev. A **64**, 012304.
10. Zhao Z, Yang T, Chen Y A, Zhang A N and Pan J W 2003 Phys. Rev. Lett. **90**, 207901.
11. Yamamoto T, Koashi M, Ozdemir S K and Imoto N 2003 Nature **421**, 343.
12. Sheng Y B, Deng F G and Zhou H Y 2008 Phys. Rev. A **77**, 062325.
13. Sheng Y B, Deng F G and Zhou H Y 2010 Quantum Inf. Comput. **10**, 272.
14. Wang C, Zhang Y and Jin G S 2011 Phys. Rev. A **84**, 032307.
15. Sheng Y B, Zhou L, Zhao S M and Zheng B Y 2012 Phys. Rev. A, **85**, 012307.
16. Deng F G 2012 Phys. Rev. A, **85**, 022311.
17. Gaebel T, et al. 2006 Nature Physics, **2**, 408.
18. Duan L M, Wang B, and Kimble H J 2005 Phys. Rev. A, **72**, 032333.
19. An J H, Feng M, Oh C H 2009 Phys. Rev. A, 79, 032303.
20. Yang W L, Xu Z Y, Feng M and Du J F 2010 New J. Phys. **12**, 003039.
21. Yang W L, Yin Z Q, Hu Y, Feng M and Du J F 2011 Phys. Rev. A **84**, 010301(R).
22. Dayan B, Parkins A S, Aoki T, Ostby E P, Vahala K J and Kimble H J 2008 Science, 319, 1062.
23. Chen Q, Yang W L, Fang M and Du J F 2011 Phys. Rev. A, 83, 054305.

24. Li P B, Gao S Y, Li F L 2011 Phys. Rev. A, 83, 054306.
25. Yu X C, Liu Y C, Yan M Y, Liu W L, and Xiao Y F 2012 Phys. Rev. A, 86, 043833.
26. Jiang L, et al. 2009 Science, 326, 267.
27. Togan E, et al. 2010 Nature, 466, 730.
28. Buluta I, Ashhab S, and Nori F, 2011 Rep. Prog. Phys. 74 104401
29. Buluta I, and Nori F, 2009 Science 326, 108
30. You J Q, and Nori F, 2005 Phys. Today, 58(11), 42-47
31. You J Q, and Nori F, 2011 Nature, 474, 589.
32. Nation P D, Johansson J R, Blencowe M P, and Nori F, 2012 Rev. Mod. Phys., 84, 1-24.
33. Zhou L, Gong Z R, Liu Y X, Sun C P, and Nori F, 2008 Phys. Rev. Lett., 101, 100501.
34. Zhou L, Dong H, Liu Y X, Sun C P and Nori F, 2008 Phys. Rev. A, 78, 063827
35. Zhou L, Yang S, Liu Y X, Sun C P and Nori F, 2009 Phys. Rev. A, 80, 062109
36. Liao J Q, Gong Z R, Zhou L, Liu Y X, Sun C P and Nori F, 2010 Phys. Rev. A, 81, 042304
37. Maunz P, et al. 2007 Nat. Phys., 3, 538.
38. Schmid S I and Evers J 2011 Phys. Rev. A, 84, 053822.
39. Walls D F and Milburn G J 1994 Quantum Optics (Springer-Verlag,Berlin Heidelberg).
40. De Lange G, Wang Z H, Riste D, Dobrovitski V V, and Hanson R, 2010 Science, 330, 60-63
41. Park Y S, Cook A K and Wang H, 2006 Nano Lett. 6, 2075.
42. Barclay P E, Fu F M C, Santori C and Beausoleil R G 2009 App. Phys. Lett., 95, 191115.
43. Englund D, Shields B, Rivoire K, Hatami F, Vuckovic J, Park H and Lukin M D 2010 Nano Lett., 10 (10), 3922.
44. Aoki T, Parkins A S, Alton D J, Regal C A, Dayan B, Ostby E, Vahala K J and Kimble H J 2009 Phys. Rev. Lett., 102, 083601.
45. Barclay P E, Santori C, Fu F -M , Beausoleil R G and Painter O 2009 Optics Express, 17, 8081.
46. Neumann P, Mizuochi N, Rempp F, Hemmer P, et al. 2008 Science, 320, 1326.
47. Balasubramanian G, et al. 2009 Nature Materials, 8, 383.
48. Wang C, Zhang Y, Jin G S, and Zhang R, 2012 J. Opt. Soc. Am. B, 29(12), 3349-3354.